Journal of Alloys and Compounds, 200 (1993) 99–105
JALCOM 772

Phase diagram and electrical behavior of silicon-rich iridium silicide compounds

C.E. Allevato and Cronin B. Vining
Jet Propulsion Laboratory–California Institute of Technology, Pasadena, CA 91109 (USA)

(Received December 28, 1992; in final form April 6, 1993)

Abstract

The iridium–silicon phase diagram on the silicon-rich side was investigated by means of X-ray powder diffraction, density, differential thermal analysis (DTA), metallography, microprobe analysis, and electrical resistivity. Attempts were made to prepare eight previously reported silicon-rich iridium silicide compounds by arc melting and Bridgman-like growth. However, microprobe analysis identified only five distinct compositions: IrSi, Ir_4Si_5, Ir_3Si_4, Ir_3Si_5 and $IrSi_{\approx 3}$. The existence of Ir_2Si_3, Ir_4Si_7, and $IrSi_2$ could not be confirmed in this study. DTA in conjunction with X-ray powder diffraction confirm polymorphism in $IrSi_{\approx 3}$, determined to have orthorhombic and monoclinic unit cells in the high and low temperature forms. A eutectic composition alloy of 80.5 ± 1 at.% Si was observed between $IrSi_{\approx 3}$ and silicon. Both Ir_4Si_5 and Ir_3Si_4 exhibit distinct metallic behavior while Ir_3Si_5 is semiconducting. IrSi and $IrSi_{\approx 3}$ exhibit nearly temperature-independent electrical resistivities on the order of $(5–10) \times 10^{-6}$ Ω m.

1. Introduction

The transition metal silicides form a series of refractory compounds [1] ranging in chemical bonding from metallic to covalent, suggesting a great variety of interesting physical properties. Some of these compounds may be of particular interest for microelectronic or thermoelectric [2] applications. Unfortunately, the phase diagram has not yet been determined and most of the work involving iridium silicides deals with non-equilibrium thin films. The current study focused on silicon-rich materials in order to identify which, if any, of the compounds in the Ir–Si system might be of interest for thermoelectric applications.

According to Finnie [3], the Ir–Si system is mostly in the solid state at 1610 K and seven phases could be identified by X-ray diffraction [4]. Nicolet and Lau [5] describe more than eight intermediate phases. More recent investigations by Petersson *et al.* [6] and Wittmer *et al.* [7] of the interaction of iridium films with silicon substrates revealed the existence of only three distinct phases: (1) IrSi observed between 673 K and 873 K; (2) a phase with composition close to Ir_4Si_7 observed from 773 K to 1223 K; (3) $IrSi_{\approx 3}$ observed at temperatures in the vicinity of 1273 K.

Petersson *et al.* [8], Bost and Mahan [9] and Frampton and Irene [10] suggest that the compound identified as Ir_4Si_7 is a semiconductor. Engström *et al.* [11] determined the correct composition of this compound as Ir_3Si_5 by single-crystal X-ray diffraction studies.

In contrast to the semiconducting behavior in Ir_3Si_5, White and Hockings [12] and Bhan and Schubert [13] report that iridium trisilicide, $IrSi_{\approx 3}$, has a metal-like resistivity and a hexagonal crystal structure. Engström and Zdansky [14] investigated polycrystalline, arc-melted $IrSi_{\approx 3}$ and found an orthorhombic crystal structure which, after heat treatment for one week at 1173 K, transformed to a monoclinic form. Subsequent heat treatment at 1273 K reversed the phase transition. The reported metal-like behavior of $IrSi_{\approx 3}$ is surprising considering the unusually high silicon content of this compound.

The existence of other compounds such as Ir_4Si_5 [15], Ir_2Si_3 [6, 15, 16] and even $IrSi_2$ [17–19] has been suggested, but nothing is known concerning their transport behavior. The rule of 14 valence electrons per metal discussed by Jeitschko and Parthé [20] predicts that the composition Ir_4Si_5 should be a semiconductor. Although the structure reported for Ir_4Si_5 [15] is distinct from the structure class discussed by Jeitschko and Parthé, valence electron counting nevertheless suggests that one or more of the silicon-rich iridium silicides might be semiconducting.

2. Experimental details

The aim of this investigation is to verify the existence of eight silicon-rich iridium silicide compounds previously noted in the open literature. Samples were

0925-8388/93/$6.00

© 1993 – Elsevier Sequoia. All rights reserved

prepared by arc melting on a water-cooled copper hearth and using a two-zone graphite heating element furnace with pyrolytic boron nitride crucibles.

Arc-melted samples were prepared from high purity (99.95%), −60 mesh iridium powder, premelted into beads of approximately 4 g each. Silicon was obtained from single-crystal wafers cut into small pieces. Specimens were produced by melting stoichiometric amounts of pure iridium and silicon and were remelted two or three times in an argon-filled arc furnace. The following nominal compositions were prepared with weight losses less than 0.9%: IrSi, Ir_4Si_5, Ir_3Si_4, Ir_2Si_3, Ir_3Si_5, Ir_4Si_7, $IrSi_2$ and $IrSi_{\approx 3}$. Compositions identified as distinct phases in the arc-melted samples were afterward prepared by Bridgman-like growth under 2 lbf in^{-2} helium pressure. One sample with 57 at.% Si was obtained by quenching from the melt in a boron nitride crucible. Also, four samples with 63.5, 65.5, 70 and 75 at.% Si were prepared by arc melting and annealed at 1423 K for 7 days.

Samples were mounted, polished and examined under an optical phase contrast microscope. Microprobe analyses were determined with a Jeol superprobe using the Ir L line and the Si K line at 20 keV. Results were calculated by the Caltech ZAF program. The compound Ir_3Si_5 was used as a standard with an accuracy greater than ±1% for the specific elements of iridium and silicon. A study of the amount of different phases in each sample was acquired by using a Kevex Delta energy dispersive analyzer of X-rays in conjunction with feature analysis.

A semiquantitative determination of impurities was determined for two samples of IrSi using a laser ion mass spectroscopy technique and oxygen and nitrogen content was determined on the same two samples using an inert gas fusion technique.

The critical temperature of each sample was determined by differential thermal analysis (DTA) in a DuPont 1600 °C DTA furnace using pyrolytic boron nitride crucibles and argon as the purge gas. The boron nitride crucibles delaminated during cycling but otherwise functioned satisfactorily and were non-reactive with the samples. The heating rate was 25 K min^{-1} up to 1123 K and 10 K min^{-1} to a temperature greater than the melting point, except for the IrSi sample which had a melting point higher than the upper limit of the DTA furnace of 1873 K. The DTA instrument, calibrated using pure gold and silicon samples as standards, has an estimated uncertainty of less than ±10 K.

The melting points of four samples were also determined by an independent, near-equilibrium method using the Bridgman growth furnace. Control temperatures, determined by optical pyrometry, were calibrated using W–5%Re/W–26%Re thermocouples and by melting high purity standards of elemental silicon, germanium and platinum. Only small corrections (±15 K) were required. Iridium silicide samples were heated in boron nitride crucibles under helium gas, cooled to room temperature and examined visually. If the sample had not melted, the procedure was repeated at a higher temperature until the entire sample had melted. Melting points determined by this method were in agreement with DTA results to within 15 K for three samples determined by both methods.

Density measurements were performed in toluene by the Archimedes method and all density values were repeatable to within 0.5%. A Siemens D-500 diffractometer with Cu $K\alpha$ radiation was used to obtain powder X-ray patterns with a step scan interval in 2Θ of 0.05° and a 7 s count time. Electrical resistivity measurements were performed by means of the van der Pauw method [21] from 300 to 1330 K, neglecting any anisotropy effects.

3. Results and discussion

Results obtained with the above techniques are summarized in Table 1 and in the phase diagram of Fig. 1. Five distinct phases were observed to form in quantities detectable by microprobe analysis. In the following section, we discuss the various results in more detail.

3.1. *IrSi*

Single-phase iridium monosilicide was obtained by arc melting stoichiometric amounts of the elements and also by Bridgman growth with an initial composition corresponding to Ir_4Si_5. Typically, IrSi grains exhibit striation-like defects clearly visible in optical micrographs. Microprobe analysis of the arc-melted sample revealed only trace amounts of Ir_2Si (less than 1%). Several attempts to grow crack-free IrSi by the Bridgman method were unsuccessful. IrSi obtained by arc melting had an X-ray powder diffraction pattern, lattice parameters and density consistent with the orthorhombic form previously reported. However, IrSi obtained by the Bridgman method exhibited slight shifts of several X-ray lines, as shown in Fig. 2. Table 2 indicates that the X-ray pattern of this sample can be indexed assuming an orthorhombic unit cell, but with lattice parameters slightly different from previous results [15, 22].

X-ray powder diffraction line intensities were calculated for each of these samples assuming the MnP-type structure (space group *Pnma*) and atomic positions (iridium at $x=0.005$, $y=0.250$, $z=0.200$ and silicon at $x=0.190$, $y=0.250$, $z=0.570$) suggested by Korst *et al.* [22]. Measured and calculated intensities correspond only approximately, yielding a figure of merit coefficient $R=0.26$ and $R=0.33$ for the arc-melted and Bridgman-grown samples respectively. Adjusting the atomic po-

TABLE 1. Intermediate phases in the silicon-rich portion of the iridium silicide system

Phase	Structure type	Reference	Composition (at.% Si)	Density (g cm^{-3})		Temperature (K)	Resistivity[a] ($\times 10^{-8}$ Ω m)
				Calculated	Experimental		
IrSi	MnP	[15]	50.1 ± 0.5	13.00	12.51 ± 0.06	1980 ± 15	500
Ir_4Si_5	Rh_4Si_5	[15]	55.7 ± 0.6	11.67	11.65 ± 0.06	1588 ± 10	74
Ir_3Si_4	Rh_3Si_4	[15]	57.0 ± 0.6	11.36	10.89 ± 0.05	1681 ± 10	60
Ir_3Si_5	Ir_3Si_5	[11]	62.5 ± 0.6	10.17	10.12 ± 0.05	1675 ± 10	59300
$IrSi_{\approx 3}$(o)	Orthorhombic	[14]	72.5 ± 0.7	8.44	8.21 ± 0.04	1533 ± 10	350
$IrSi_{\approx 3}$(m)	Monoclinic	[14]	–	8.43	–	1248 ± 10	580

[a]Room temperature.

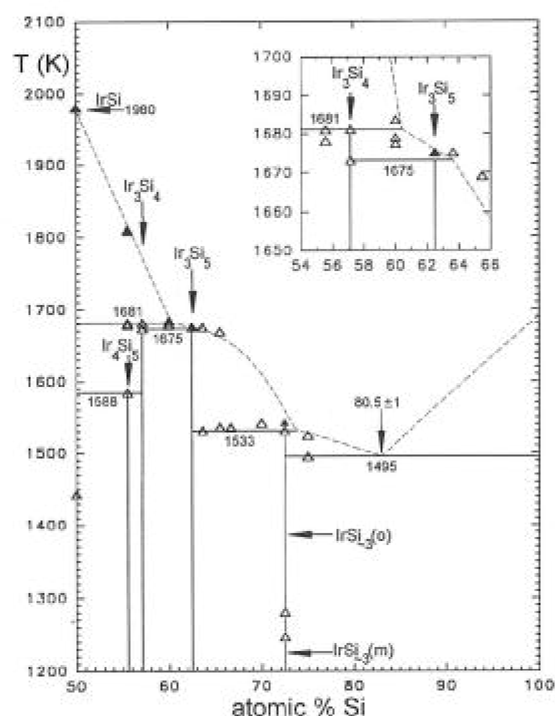

Fig. 1. Partial iridium silicon phase diagram: △, determined by DTA; ▲, determined by direct observation.

sitions of iridium and silicon did not significantly improve the agreement, yielding $R = 0.24$ and $R = 0.31$ respectively.

Chemical analysis indicated that the arc-melted IrSi sample contained 0.06% O and the Bridgman-grown sample contained 0.47% O, 0.30% C, 0.29% N, and 0.01% B, each on an atomic basis. No other impurities were detected at concentrations greater than 20 at.ppm.

DTA carried out up to 1673 K revealed a significant transition at 1443 K. The melting point of 1980 K for IrSi was obtained by the visual observation method described above. IrSi is presumed to melt congruently, as suggested by the Ir_2Si traces detected, as described above.

The electrical resistivity of the arc-melted IrSi sample, shown in Fig. 3, is only weakly temperature dependent. The resistivity increases from 4.5×10^{-6} Ω m at 300 K to a maximum of 5.6×10^{-6} Ω m at 950 K, after which the resistivity decreases to 5.1×10^{-6} Ω m at 1300 K.

3.2. Ir_4Si_5

The compound Ir_4Si_5 was not observed in as-prepared samples, but, after annealing an arc-melted sample with nominal composition of Ir_4Si_5 at 1523 K for 7 days, only a single phase was observed by microprobe analysis. The composition, density and X-ray powder pattern of this phase correspond to the compound Ir_4Si_5 reported by Engström and Zackrisson [15]. DTA indicated a transition at 1588 K, consistent with peritectoidal decomposition as indicated in the phase diagram in Fig. 1. The electrical resistivity of Ir_4Si_5 indicates metallic behavior, as shown in Fig. 3.

3.3. Ir_3Si_4

Microprobe analysis on as-prepared samples identified only one phase between IrSi (50% Si) and Ir_3Si_5 (62.5% Si). The density, composition determined by microprobe ($57.0\% \pm 0.5\%$ Si) and the X-ray powder diffraction pattern are in excellent agreement with the Ir_3Si_4 compound reported by Engström and Zackrisson [15]. Neither microprobe nor X-ray diffraction yielded any evidence for the compound Ir_4Si_5, except after annealing as described above.

Arc-melted samples, with nominal compositions Ir_4Si_5, Ir_3Si_4 and Ir_2Si_3, as prepared exhibit a dendritic microstructure, becoming less dense with increasing silicon content, as shown in Fig. 4. A typical eutectic microstructure was not observed in this composition range. Microprobe analysis indicates the dendrite core to be IrSi surrounded by Ir_3Si_4 in an Ir_3Si_5 matrix. The electrical resistivity of the Ir_3Si_4 compound was 6×10^{-7} Ω m at 300 K and exhibited an increase with increasing temperature (Fig. 3), typical of metals.

3.4. Ir_3Si_5

Single-phase, polycrystalline Ir_3Si_5 was prepared by arc melting with density and X-ray patterns in good

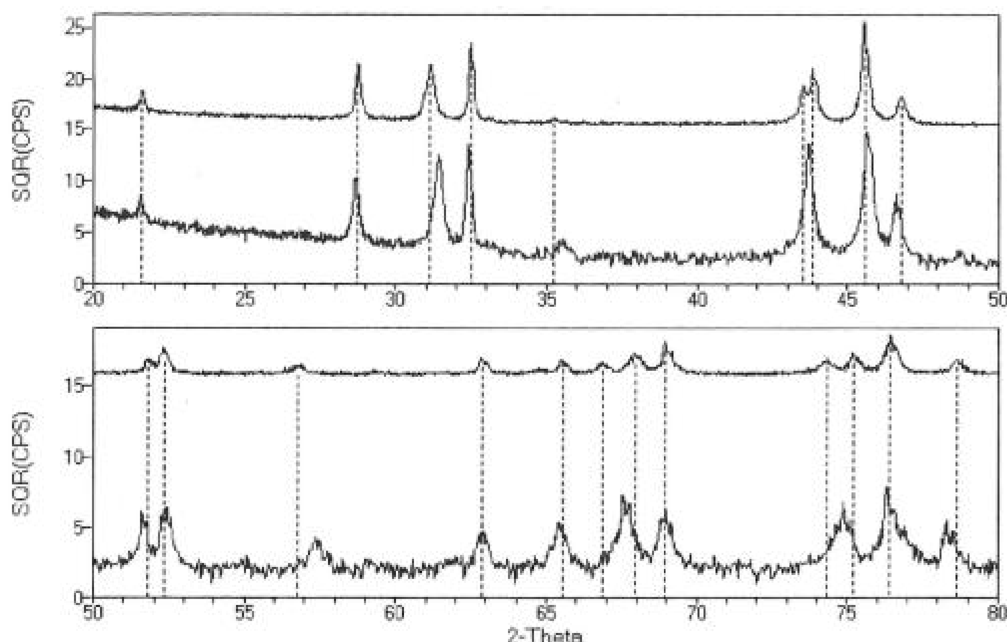

Fig. 2. X-ray diffraction patterns of IrSi prepared by arc melting (lower curve) and by Bridgman growth (upper curve).

TABLE 2. IrSi lattice parameters

Sample	*a* (Å)	*b* (Å)	*c* (Å)	Volume (Å³)
Korst *et al.* [22]	5.558(5)	3.211(5)	6.273(5)	112.0
Engström and Zackrisson [15]	5.558(3)	3.221(3)	6.267(1)	112.2
This study, arc melted	5.555(1)	3.215(1)	6.267(1)	111.9
This study, Bridgman grown	5.532(1)	3.247(1)	6.241(1)	112.2

agreement with the monoclinic structure reported by Engström *et al.* [11]. Attempts to grow this compound by the Bridgman method from a stoichiometric melt were not successful. Growth from a slightly silicon-rich melt (65% Si) resulted in a layer of Ir_3Si_4 compound at the bottom of the ingot, followed by a layer of Ir_3Si_5, and at the top a layer of $IrSi_{\approx 3}$. A eutectic-like microstructure was observed in a thin layer at the interface between Ir_3Si_5 and $IrSi_{\approx 3}$, as shown in Fig. 5. This eutectic-like microstructure was not observed in any other samples and has been attributed to non-equilibrium growth conditions. A better Bridgman-grown sample was achieved by first arc melting the silicon-rich charge (65% Si) in order to homogenize the melt.

The arc-melted sample of Ir_3Si_5 exhibited no trace of a eutectic-like microstructure and DTA indicated melting at 1675 K. DTA of a sample with nominal composition of Ir_4Si_7 revealed two major transitions at 1604 K and at 1675 K. The transition at 1604 K may be due to non-equilibrium within the sample or may indicate a homogeneity range which depends on temperature. Ir_3Si_5 exhibits a resistivity profile (Fig. 3) that resembles the behavior of a semiconductor and Hall effect measurements indicate the sample is p type over the entire temperature range. The resistivity at room temperature is 6×10^{-4} Ω m, increases to 1×10^{-3} Ω m at 750 K, and decreases to 1.2×10^{-4} Ω m at 1300 K, which is typical of a lightly doped semiconductor.

3.5. $IrSi_{\approx 3}$

Slightly higher weight losses, around 1.3%, resulted when arc melting a 75% Si sample compared with less silicon-rich compositions. A eutectic structure consisting of $IrSi_{\approx 3}$ and pure silicon was observed by microprobe analysis with a composition of 80.5% ± 1% Si, as shown in Fig. 6. DTA indicated a transition at 1495 K, consistent with the eutectic temperature shown in Fig. 1.

A single-phase sample of $IrSi_{\approx 3}$ was obtained by the Bridgman technique from a 75% Si melt, with evidence of a eutectic alloy only at the top of the ingot. DTA and visual observation of a single-phase portion of this sample indicate melting at about 1533 K. DTA also provided evidence of small transitions at 1248 K and 1281 K, consistent with the existence of polymorphism as suggested by Engström and Zdansky [14]. X-ray powder diffraction on the as-prepared Bridgman-grown

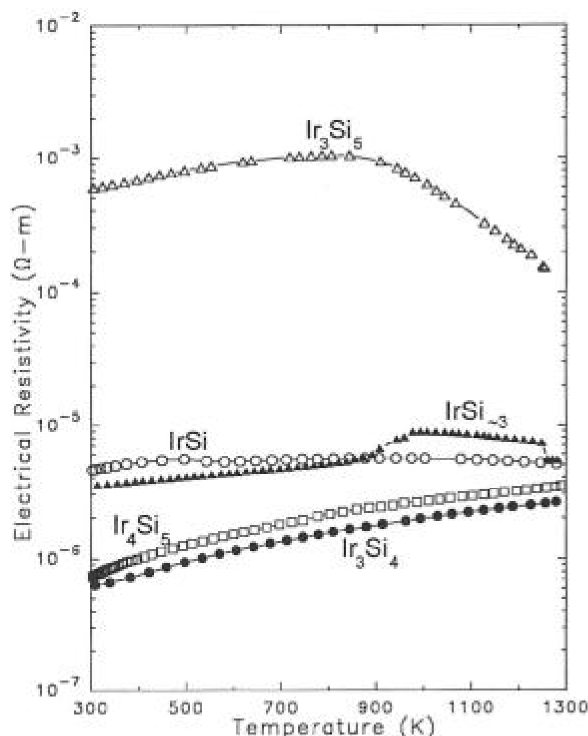

Fig. 3. Electrical resistivity as a function of temperature for five iridium silicides.

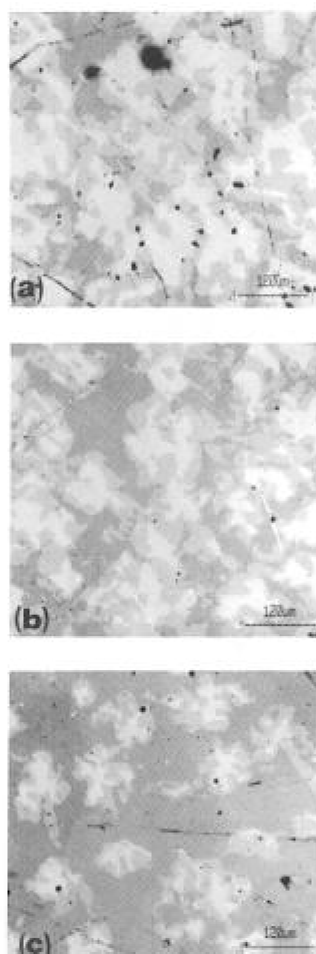

Fig. 4. Micrographs showing dendrites observed in as-prepared arc-melted samples with various nominal compositions: (a) Ir_4Si_5 (34% IrSi, 46% Ir_3Si_4, 20% Ir_3Si_5); (b) Ir_3Si_4 (24% IrSi, 44% Ir_3Si_4, 32% Ir_3Si_5); (c) Ir_2Si_3 (10% IrSi, 23% Ir_3Si_4, 67% Ir_3Si_5).

sample of $IrSi_{\sim3}$ agreed reasonably well with the pattern reported by Engström and Zdansky [14] for the orthorhombic form, $IrSi_{\sim3}$(o), although a few additional peaks were observed. Engström and Zdansky [14] suggest that the true stoichiometry corresponds to a composition of 74% Si. Microprobe analysis performed in the present work on this phase leads to the value of $72.5\% \pm 0.7\%$ Si, which again is slightly less than the ideal trisilicide composition. The experimental density of 8.20 g cm^{-3} is in close agreement with the theoretical density of 8.48 g cm^{-3} indicated by Finnie [3], as well as with an experimental value of 8.64 g cm^{-3} reported by Bhan and Schubert [13].

Electrical resistivity measurements performed on Bridgman-grown $IrSi_{\sim3}$, shown in Fig. 3, indicate two relatively sharp features. The resistivity slowly increases with increasing temperature. Between 900 K and 1000 K the resistivity increases rapidly to a maximum of 8.9×10^{-6} Ω m at about 1000 K. Then, the resistivity slowly decreases with further increase in temperature and at 1265 K the resistivity suddenly drops by about 35% to 5.5×10^{-6} Ω m. The sudden change in resistivity observed at 1265 K is presumed to be related to similar features observed by DTA at 1248 and 1281 K.

On cooling, the resistivity exhibited significant hysteresis (not shown) and returned to a room temperature resistivity value of 5.8×10^{-6} Ω m, significantly above the room temperature value of 3.5×10^{-6} Ω m observed in the as-prepared state. The X-ray diffraction pattern also changed after thermal cycling and agreed quite well with the monoclinic $IrSi_{\sim3}$(m) pattern reported by Engström and Zdansky [14]. No features were observed by DTA performed on this sample.

$IrSi_{\sim3}$(o) has been observed only in as-prepared samples, both in this study and by Engström and Zdansky [14]. Presumably this is the high temperature form and $IrSi_{\sim3}$(m) is the stable low temperature form. At the beginning of the resistivity measurements, the Bridgman-grown $IrSi_{\sim3}$ sample was frozen in the orthorhombic form. The rapid increase in resistivity between 900 and 1000 K may represent transformation to the more stable monoclinic form. Similarly, the sharp decrease in resistivity at about 1265 K may represent return of the sample to the orthorhombic form, which appears to be the stable form above this temperature.

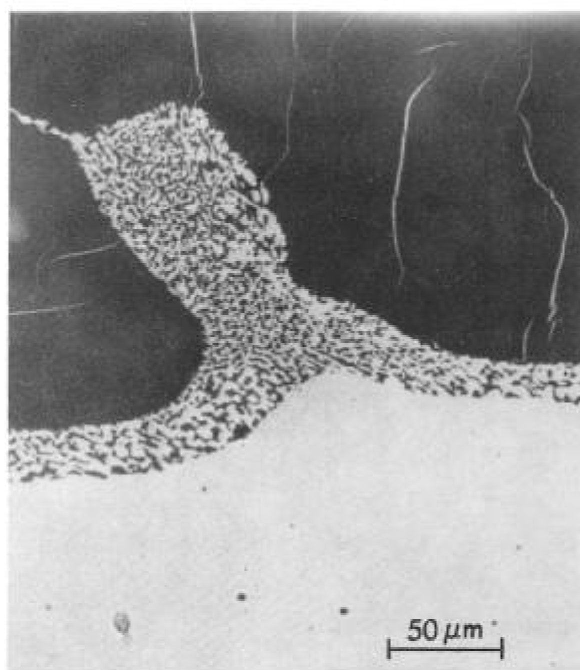

Fig. 5. Eutectic-like microstructure observed at the interface between Ir_3Si_5 (light) and $IrSi_{\approx 3}$ (dark), attributed to non-equilibrium growth conditions.

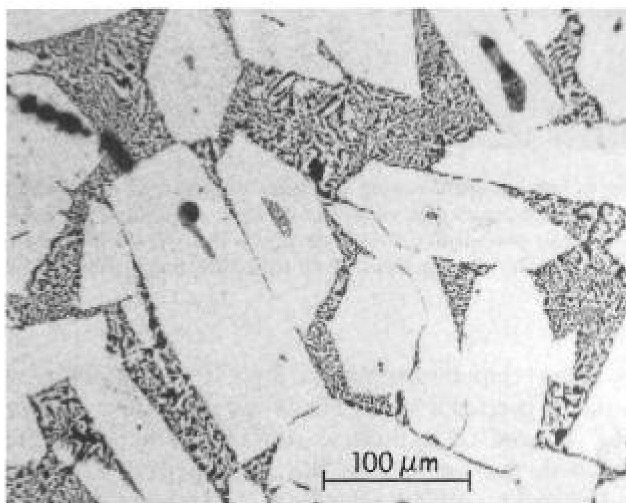

Fig. 6. Eutectic composition alloy showing the intimate mixture of $IrSi_{\approx 3}$ (light) and silicon (dark).

4. Conclusion

The present investigation allowed for the first time determination of the Ir–Si phase diagram on the silicon-rich side. The monosilicide melts at 1980 K, presumably congruently, and exhibits metallic conduction. Impurities appear to alter slightly the lattice parameters of IrSi, consistent with a previous report of lattice parameter variations when IrSi is prepared in a boron nitride crucible [3]. The relatively poor agreement between calculated and observed X-ray powder diffraction line intensities ($R \approx 0.24$–0.33) reported in this study and similar results reported for the isostructural RhSi compound [23] indicate that the description of the crystal structure for these materials is incomplete and more definitive single-crystal X-ray studies are required.

The existence of Ir_4Si_5 was confirmed with a peritectoid formation temperature of 1588 K. The existence of Ir_3Si_4 was confirmed with a peritectic formation temperature of 1681 K. Both compounds exhibit metallic conduction. A peritectic formation temperature of 1675 K was determined for Ir_3Si_5 and p-type semiconducting behavior of this compound was confirmed.

The most silicon-rich compound in the Ir–Si system, indicated as $IrSi_{\approx 3}$, has a composition of about 72.5% Si, a peritectic decomposition temperature of 1533 K and transforms from a high temperature orthorhombic structure to a low temperature monoclinic structure at about 1248 K. Both forms exhibit semimetallic or heavily doped semiconducting behavior.

Several features of the Ir–Si phase diagram require further study, such as polymorphism in $IrSi_{\approx 3}$ and possibly IrSi. Also, the iridium-rich side of the Ir–Si system remains to be determined.

Acknowledgments

The work described in this paper was carried out at the Jet Propulsion Laboratory, California Institute of Technology, under contract with the National Aeronautics and Space Administration. The authors wish to express their gratitude to Professor B.T. Fultz of the California Institute of Technology for providing access to arc melting facilities, P. Carpenter for the microprobe analysis, L. Lowry and J. Kulleck for the X-ray patterns, R. Ruiz for energy-dispersive X-ray results, J. McCormack for the Hall effect measurements, and G. Hickey for the DTA. The authors also wish to thank R. Conzemius of the Materials Preparation Center at Ames, IA, for performing the chemical analyses.

References

1 K.N. Mason, *Prog. Cryst. Growth Charact.*, *2* (1979) 269.
2 A.W. Searcy and D.J. Mesch, in P.H. Egli (ed.), *Thermoelectricity*, Wiley, New York, 1960, p. 159.
3 L.N. Finnie, *J. Less-Common Met.*, *4* (1962) 24.
4 K. Schubert, S. Bhan, W. Burkhardt, R. Gohle, H.G. Meissner, M. Potzschke and E. Stoltz, *Naturwissenschaften*, *47* (1960) 303.
5 M.A. Nicolet and S.S. Lau, in N.G. Einspruch and G.B. Larrabee (eds.), *VLSI Electronics: Microstructure Sciences*, Academic Press, New York, 1983, p. 329.

6 S. Petersson, J. Baglin, W. Hammer, F. d'Heurle, T.S. Kuan, I. Ohdomary, J. de Souza Pires and P. Tove, *J. Appl. Phys., 50*(5) (1978) 3357.

7 M. Wittmer, P. Oelhafen and K.N. Tu, *Phys. Rev. B, 35*(17) (1987) 9073.

8 S. Petersson, J.A. Reimer, M.H. Brodsky, D.K. Campbell, F. d'Heurle, B. Karlsson and P.A. Tove, *J. Appl. Phys., 53*(4) (1982) 3342.

9 M.C. Bost and J.E. Mahan, *J. Vac. Sci. Technol. B, 4*(6) (1986) 1336.

10 R.D. Frampton and E.A. Irene, *J. Appl. Phys., 59*(3) (1986) 978.

11 I. Engström, T. Sindsten and E. Zdansky, *Acta Chem. Scand. A, 41* (1987) 237.

12 J.G. White and E.F. Hockings, *Inorg. Chem., 10*(9) (1971) 1934.

13 S. Bhan and K. Schubert, *Z. Metallkd., 51* (1960) 327.

14 I. Engström and E. Zdansky, *Acta Chem. Scand. A, 36*(10) (1982) 857.

15 I. Engström and F. Zackrisson, *Acta Chem. Scand., 24* (1970) 2109.

16 I. Ohdomari, T.S. Kuan and K.N. Tu, *J. Appl. Phys., 50*(11) (1979) 7020.

17 B.Z. Weiss, K.N. Tu and D.A. Smith, *J. Appl. Phys., 59*(2) (1986) 415.

18 J.H. Buddery and A.J. Welch, *Nature (London), 167* (1951) 362.

19 K. Schubert and S. Bhan, *Naturwissenschaften, 47* (1960) 303.

20 W. Jeitschko and E. Parthé, *Acta Crystallogr., 22* (1967) 417.

21 J. McCormack and J.-P. Fleurial, *Mater. Res. Soc. Symp. Proc., 234* (1991) 135.

22 W.L. Korst, L.N. Finnie and A.W. Searcy, *J. Phys. Chem., 61* (1957) 1541.

23 L. Schellenberg, J.L. Jorda and J. Muller, *J. Less-Common Met., 109* (1985) 261.